How to cite: *Angew. Chem. Int. Ed.* **2023**, *62*, e202302318
doi.org/10.1002/anie.202302318

Biophysical Chemistry

Controlled Grafting Expansion Microscopy

Ria Thielhorn[+], Isabelle Heing-Becker[+], Nadja Hümpfer, Jakob Rentsch, Rainer Haag, Kai Licha, and Helge Ewers**

Abstract: Expansion microscopy (ExM) is a recently developed technique that allows for the resolution of structures below the diffraction limit by physically enlarging a hydrogel-embedded facsimile of the biological sample. The target structure is labeled and this label must be retained in a relative position true to the original, smaller state before expansion by linking it into the gel. However, gel formation and digestion lead to a significant loss in target-delivered label, resulting in weak signal. To overcome this problem, we have here developed an agent combining targeting, fluorescent labeling and gel linkage in a single small molecule. Similar approaches in the past have still suffered from significant loss of label. Here we show that this loss is due to insufficient surface grafting of fluorophores into the hydrogel and develop a solution by increasing the amount of target-bound monomers. Overall, we obtain a significant improvement in fluorescence signal retention and our new dye allows the resolution of nuclear pores as ring-like structures, similar to STED microscopy. We furthermore provide mechanistic insight into dye retention in ExM.

Introduction

Overcoming the diffraction-limit of light by the development of super-resolution microscopy (SRM) techniques has revolutionized fluorescence imaging, especially in the life sciences. In contrast to other SRM methods, expansion microscopy (ExM) enables sub-diffraction imaging using conventional fluorescence microscopes.[1] Here, biological structures are fluorescently labeled and the labels are linked to a swellable hydrogel that is formed throughout the sample. When the hydrogel is subsequently expanded by the addition of pure water, the labels are physically pulled apart while maintaining their relative position to one another. Ultimately, this results in a significantly and isotropically enlarged facsimile of the original structure. Fluorophores that were originally too close to each other to be resolved can now be detected separately from each other, resulting in a superresolved image of the native structure. In this way, super-resolution imaging can be performed for a broader range of users and samples with conventional labeling techniques and existing microscopy technology.[2] Further improvement in resolution has been demonstrated by combining ExM with other modes such as stimulated emission depletion (STED) microscopy,[3,4] structured illumination microscopy (SIM)[5] and single molecule localization microscopy (SMLM).[6]

However, important challenges for ExM remain to be addressed. One major issue is a strong loss of fluorescence intensity. First, the local fluorophore density is necessarily decreased by the physical expansion of the gel into all three spatial dimensions. Secondly, some fluorophores, e.g. cyanine dyes, cannot withstand the chemistry of the polymerization process.[7,8] Thirdly, if proteolytic digestion of the sample cuts between the dye and the target structure, the specific labeling may be lost. As a result, antibody fragments carrying a dye or parts of enzymatic labels such as SNAP-tag may be cut off and diffuse away.

The first problem is an intrinsic tradeoff to the resolution-enhancement in ExM. The second problem can be averted by the choice of dye[1,7,9] or by delivering the dye after gel formation.[7,10,11] The third problem is more difficult to handle and an active area of research. Amine-reactive reagents like AcX (6-((acryloyl)amino)hexanoic acid succinimidyl ester) or MA-NHS (methacrylic acid *N*-hydroxysuccinimide ester) are used to anchor proteins and labeling agents like antibodies or enzymatic tags to the polymer mesh by equipping them with a functional monomer group. The latter has the capability to become incorporated into the hydrogel during polymerization in a process called grafting. However, the resulting gel-anchoring points are unevenly distributed across the target structure and only the proteins, but not the dyes themselves, are linked to the hydrogel. The enzymatic digestion of the sample thus may result in the formation of different types of fragments (Figure 1a) that remain visible in microscopy only when they are covalently linked both to the hydrogel and to the dye simultaneously. Other fragments will be washed away or remain without dye.

[*] R. Thielhorn,[+] N. Hümpfer, J. Rentsch, H. Ewers
Institut für Chemie und Biochemie, Freie Universität Berlin
Thielallee 63, 14195 Berlin (Germany)
E-mail: helge.ewers@fu-berlin.de

I. Heing-Becker,[+] R. Haag, K. Licha
Institut für Chemie und Biochemie, Freie Universität Berlin
Takustr. 3, 14195 Berlin (Germany)
E-mail: kai.licha@fu-berlin.de

[+] These authors contributed equally to this work.

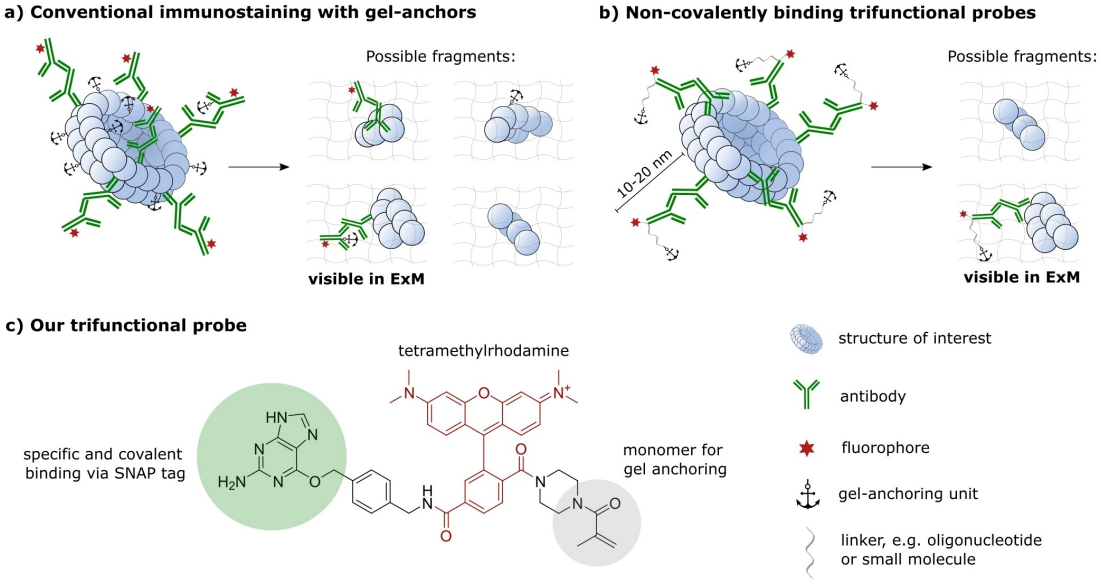

Figure 1. Different concepts for pre-labeling ExM. a) Conventional ExM immunostaining results in an unspecific distribution of gel-anchoring units. Four different types of fragments are created by enzymatic digestion of the gel, some of which must lead to a loss of fluorescence signal during expansion. b) Trifunctional probes contain a fluorescent reporter, a targeting moiety and a gel-anchoring group, so that only two types of fragments should be generated. Binding to the target structure can occur via specific or unspecific, covalent or non-covalent interactions. c) Our trifunctional probe binds specifically and covalently via a SNAP-tag to the protein of interest and possesses a polymerizable monomer, which can be incorporated into the hydrogel during polymerization.

To overcome this problem, several ideas have been put forward to combine gel-anchoring, target-delivery and dye moiety in a trifunctional manner (Figure 1b).[12–15] Most of these approaches combine fluorophore and gel-anchorage with a noncovalent means of delivery and allow for better retention of fluorescence and precise labeling. We here aimed to further improve on this theme, by combining fully covalent target linkage through the widely used SNAP-tag, an acrylate moiety and a bright and stable fluorescent rhodamine dye in a <1 kDa probe (Figure 1c).

Results and Discussion

We reasoned that coupling of the dye through the SNAP-tag directly at the structure of interest and anchorage via the acrylate right at the destination would lead to a reduced labeling error[16–18] and optimal retention of dyes for brightest possible labeling. Among the different classes of organic fluorophores, we chose a rhodamine-based approach for the development of our trifunctional probe (Figure 1c). Rhodamines possess a high brightness and photostability and have proven to be robust compounds for the polymerization step during ExM.[19] They offer further functionalization possibilities via the carboxyphenyl ring, making them ideal candidates for a linker platform between a biological targeting unit and a gel-anchoring moiety. We chose the commercially available dye 6-carboxytetramethylrhodamine (TMR), which comprises an additional carboxylic acid in the carboxyphenyl ring. The carboxyl groups can be successively activated and functionalized.[20] In this context, we first attached benzylguanine (BG) via the additional carboxyl group of TMR. The BG allows for covalent and specific labeling of the protein of interest (POI) via a SNAP-tag. Furthermore, it reduces the labeling error in comparison to conventional immunostaining, where the dye is delivered several nanometers away from the original structure. We then activated the remaining carboxyl group of the rhodamine dye and attached a piperazine linked to a methacrylic (MA) monomer. Masking the carboxylic acid with a piperazine group prevents the intramolecular spirocyclization of the dye that is associated with the turn-off in its fluorescence. In principle, the introduction of the monomer group enables direct anchoring of the dye into the hydrogel and thus increases the probability of labeled fragments being copolymerized. The resulting probe, which absorbs at 565 nm and emits at 590 nm (Figure S1), is from now on termed BG-TMR-MA (benzylguanine-tetramethylrhodamine-methacrylamide).

We went on to test its stability during the ExM procedure in comparison to the commercially available SNAP-Cell TMR-Star, which bears a SNAP-tag reactive group coupled to tetramethylrhodamine, but no acrylate moiety. To do so, we measured the absorption of the dye in aqueous solution in the presence of the chemicals added during ExM (APS, TEMED, monomer solution) and after final polymerization. We found that both dyes exhibited only a small loss in absorption during the process, suggesting that TMR withstands the polymerization procedure very well (Figure 2a).

We next aimed to compare the dyes in ExM experiments to see if the acrylate moiety in our BG-TMR-MA allowed for superior dye retention compared to SNAP-Cell TMR-Star. We chose nuclear pore complexes (NPCs) as the target structure, which belong to the largest cellular protein complexes known and have been frequently used as reference

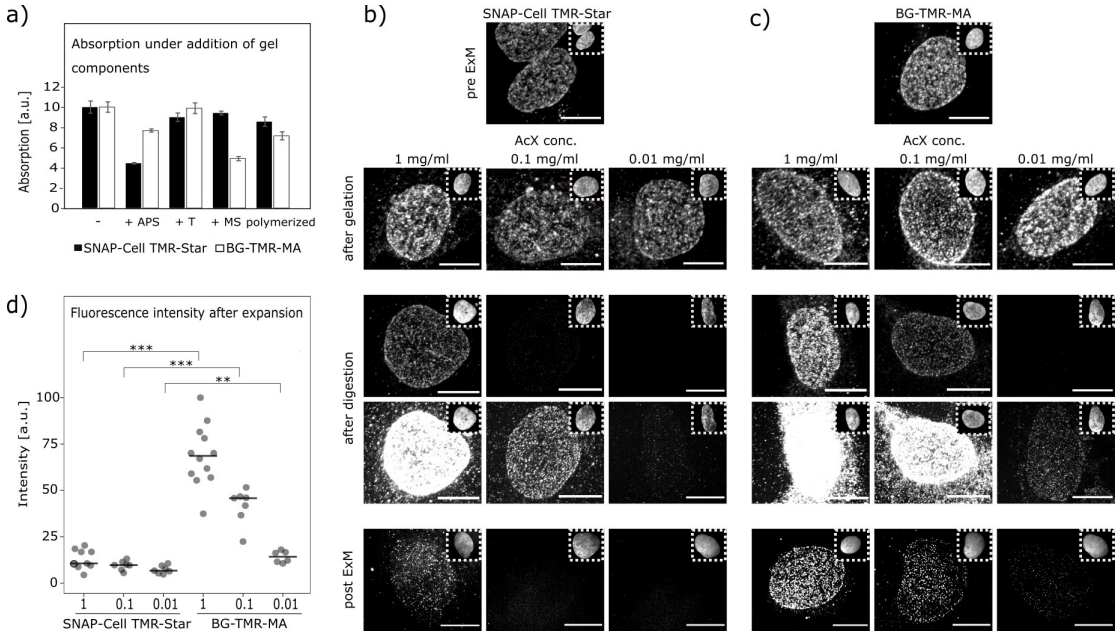

Figure 2. Comparison between SNAP-Cell TMR-Star and BG-TMR-MA. a) Relative absorption of SNAP-Cell TMR-Star and BG-TMR-MA after the addition of reagents required for the ExM protocol to simulate the effect of the chemicals on dye functionality alone. APS (ammonium persulfate), T (tetramethylethylenediamine), MS (monomer solution of acrylamide, sodium acrylate and *N*,*N*′-methylenebisacrylamide), polymerized (all reagents). Error bars represent standard deviation (SD). b) Representative confocal fluorescence micrographs of NUP96-SNAP expressing cells stained using SNAP-Cell TMR-Star after staining, gelation, digestion and expansion with different AcX concentrations. c) Representative confocal fluorescence micrographs of NUP96-SNAP expressing cells stained using BG-TMR-MA after staining, gelation, digestion and expansion with different AcX concentrations. The fluorescence micrographs imaged after digestion are shown at two different intensity-scales to emphasize the relative difference in intensity. Scaling is identical for BG-TMR-MA and SNAP-Cell TMR-Star, respectively for the top and bottom row to emphasize the relative intensity. Boxes show DAPI staining of the same cell. d) Quantification of fluorescence intensity of stained cells after expansion between SNAP-Cell TMR-Star and BG-TMR-MA after ExM in dependence of the AcX concentration. Scale bars are 10 μm.

standards due to their stereotypical structure, that appears as a ring-shape with ≈100 nm diameter that cannot be resolved in diffraction-limited microscopy.[21–24] In the cell line used for our experiments, each NPC contains 32 SNAP-tags expressed as nucleoporin 96 (NUP96) fusion proteins.[21] When performing ExM without any additional anchoring reagent, we found that indeed for SNAP-Cell TMR-Star, the fluorescence signal was undetectable. However, contrary to our expectations, we found that our BG-TMR-MA likewise led to little signal (Figure S2). Since we had tested the stability of the dye during the polymerization process, we reasoned that insufficient anchorage into the gel had to be the cause of fluorescence loss and decided to increase crosslinking during gelation with AcX, a commonly used crosslinker that is coupled randomly to free amines of sample proteins via a succinimidyl ester.

When we performed parallel ExM experiments with equal amounts of SNAP-Cell TMR-Star and BG-TMR-MA in the presence of increasing concentrations of AcX from 0.01 to 1 mg mL^{-1}, we found that with increasing AcX concentration, dye retention improved both for SNAP-Cell TMR-Star (Figure 2b) as well as for our trifunctional BG-TMR-MA (Figure 2c). Indeed, fluorescence signal was about an order of magnitude higher for BG-TMR-MA, consistent with our expectation that the acrylate moiety leads to retention of the dye in the gel (Figure 2d). To further support this hypothesis, we performed a control experiment in which we compared our probe BG-TMR-MA with the probe lacking the MA group (Figure S3). Therefore, we synthesized a probe in which the MA monomer is replaced by a Boc-protecting group. This group cannot actively participate during the polymerization step but displays a comparable size and polarity in comparison with the MA group. Similar to SNAP-Cell TMR-Star, the fluorescence intensity did not differ after staining and gelation. However, after enzymatic digestion and expansion, clear differences between BG-TMR-MA and BG-TMR-Boc were visible. These findings strongly indicate that this effect can indeed be attributed to the presence of the monomer group in our new probe. Fragments labeled with the BG-TMR-MA are anchored into the hydrogel via the polymerizable monomer of the probe and will not be washed out after enzymatic digestion, even if cleavage between the probe and a neighboring AcX anchoring point takes place. In contrast, anchoring for SNAP-Cell TMR-Star and BG-TMR-Boc is only possible via AcX, which reacts with free lysine residues of the protein of interest. Enzymatic digestion can lead to loss of labeled fragments if cleavage between the labeled part and the AcX anchorage takes place (Figure S4).

To test the quality of staining possible with our trifunctional dye, we compared its performance in ExM of nuclear pores to staining of unexpanded cells imaged by STED microscopy. We stained NUP96-SNAP cells with BG-TMR-MA in the presence of 1 mg mL^{-1} AcX and performed spinning disc confocal microscopy of the samples after

expansion by a factor of about 3 fold (Figure 3a). We could clearly detect a dip in fluorescence intensity in the center of a ring-like structure for individual nuclear pores. Pixel size in our spinning disc confocal was fixed, so that expanded samples appear pixelated in comparison to the selected 10 nm pixel size in STED scanning. Similar dips at the center of nuclear pores appeared when we stained cells via primary antibodies against NUP43-GFP and secondary antibodies coupled to Abberior Star Red and performed STED microscopy of such cells (Figure 3b). We concluded that our trifunctional dye allows for high resolution and brightness in expansion microscopy experiments when it is combined with AcX.

We next aimed to ask, whether it was sufficient to deliver AcX close to our BG-TMR-MA dye in the sample to ensure efficient incorporation. To do so, we expressed a construct of clathrin-light chain coupled to both YFP and SNAP-tag (SNAP-CLC-YFP) in cells. We then fixed these cells and stained them using our BG-TMR-MA dye in the absence of AcX. However, we then incubated the sample with AcX-coupled nanobodies directed against the SNAP-tag and YFP. We reasoned that in this way, additional moieties for linkage into the gel would be specifically delivered into close proximity of our BG-TMR-MA dye, allowing for more efficient incorporation into the gel. We hoped that such a treatment would also rescue the reduced expansion we experienced when we added 1 mg mL^{-1} of AcX to the sample (Figure S5). When we thus stained cells with BG-TMR-MA and AcX nanobodies, expanded cells and imaged them, we found that indeed the local directed delivery of AcX could rescue both BG-TMR-MA staining (Figure 4) and the expansion factor. In contrast, when the nanobodies were directed against another cellular feature, we could not.

We here demonstrated at the example of BG-TMR-MA that dyes carrying both a benzylguanine for SNAP-labeling and a monomer function can be directly crosslinked into the hydrogel polymer in ExM for better signal retention. Furthermore, our experiments point to the importance of the grafting process for signal retention in ExM. Grafting, the recruitment of growing polymer chains to a surface, and more specifically, "grafting-through", the incorporation of surface-bound monomers into a growing, grafted polymer chain,[25,26] as a process provides an explanation for our findings (Figure 5). We observed that in the absence of AcX, only little amounts of dye were retained in the gel. In this condition, our trifunctional dye provides the only available surface-bound monomers for grafting after polymerization has started in the monomer solution (Figure 5a). These dyes and thereby monomers are very sparsely distributed over the surface of the target structure and an active end of a growing polymer chain diffusing in solution is highly unlikely to collide with this insular monomer for effective chain elongation and thereby grafting.[27,28] As a result, dyes are not incorporated into the gel and lost to a great extent. We furthermore observed that the addition of AcX resulted in retention of dyes. In agreement with this observation, the efficiency of grafting increases with increasing availability of surface-bound monomers, which eventually creates conditions that can lead to "grafting-through", continuous polymerization along the surface. Grafting-through thus leads to the incorporation of trifunctional dyes (Figure 5b). Finally, using more AcX resulted in a higher fluorescence intensity. From the literature, it is known that with increasing densities of surface-bound monomers, the relative likelihood of monomer addition to occur from the surface vs. from solution increases.[25,29] The concentration of AcX thus seems to directly influence the degree to which surface-bound monomers or solute monomers become incorporated.

In this way, lower AcX concentrations can favor the formation of loops with an alternate incorporation of solute and surface-bound monomers (Figure 5b). For higher concentrations of AcX, a state could be reached, where chain growth

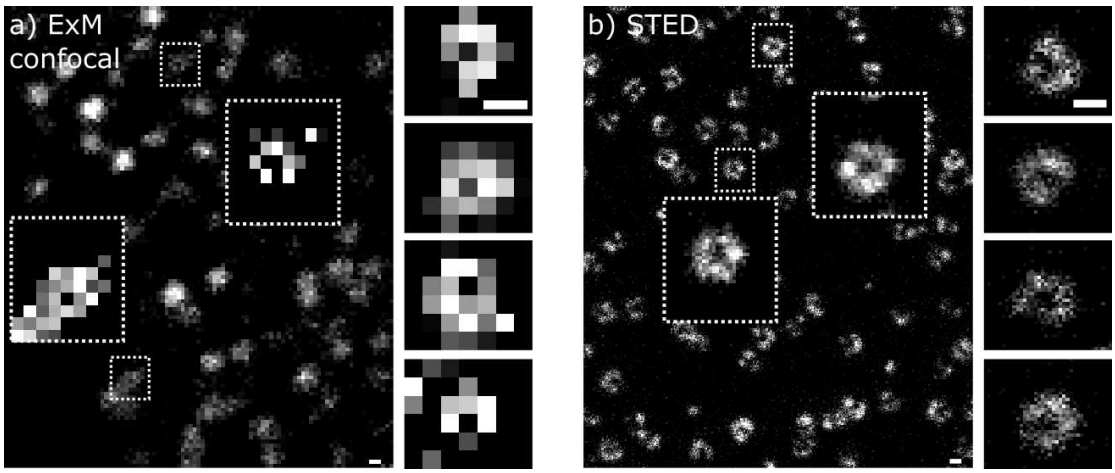

Figure 3. Comparison of super-resolution imaging modes at the example of nuclear pores. a) ExM of Nup96-SNAP labeled with BG-TMR-MA using 1 mg mL^{-1} AcX and imaged in spinning disc confocal microscopy. Insets appeared pixelated due to the fixed pixel size in spinning disc confocal microscopy of expanded sample. b) STED microscopy of nuclear pores stained through NUP43-GFP labeled with anti-GFP primary antibody, detected with an anti-mouse-Abberior Star Red secondary antibody. Zoom-in of boxed regions. On the right zoom-in images of nuclear pores taken from different cells. Scale bars are 100 nm.

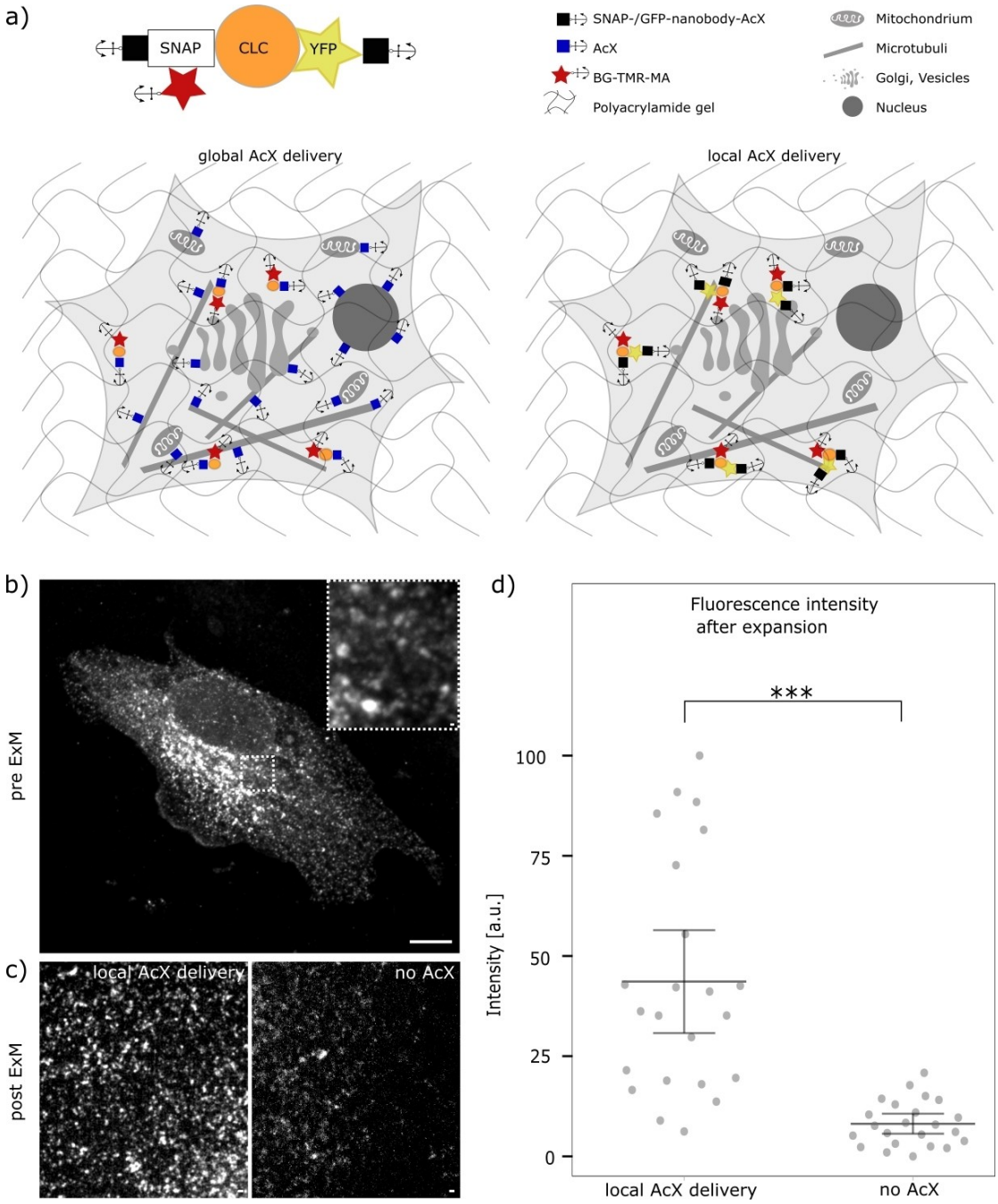

Figure 4. Local delivery of AcX leads to increased signal retention. a) Model illustrating the difference between global and local AcX delivery, using a SNAP-CLC-YFP construct and BG-TMR-MA in both cases. For global AcX delivery, AcX was used which unselectively binds to various cell structures. For local AcX delivery, AcX-coupled anti-SNAP-nanobodies and AcX-coupled anti-GFP-nanobodies were used. b) Pre-ExM confocal fluorescence micrograph of a SNAP-CLC-YFP expressing cell stained using BG-TMR-MA. Zoom-in of boxed region. c) Post-ExM zoom-in images of SNAP-CLC-YFP expressing cells with and without local delivery of AcX by AcX-coupled nanobodies. (left) BG-TMR-MA staining of SNAP-CLC-YFP in presence of AcX-coupled anti-SNAP nanobodies and AcX-coupled anti-GFP nanobodies (YFP is recognized by anti-GFP nanobody). (right) BG-TMR-MA staining of SNAP-CLC-YFP without any AcX. Scale bars are 10 µm (b), 200 nm (zoom-in b) and 200 nm (c). d) Quantification of fluorescence intensity of cells stained with BG-TMR-MA after expansion. Compared are cells ($n = 23$) without any AcX and with local delivery of AcX via AcX-coupled nanobodies. Error bars represent standard error of the mean (SEM). Tested for significance using Mann-Whitney test.

results in a mostly surface-connected in-plane polymerization. When more surface-bound polymers are incorporated, more dyes are incorporated as well, leading to a brighter fluorescent signal. This hypothesis on the importance of surface grafting for dye retention we could experimentally verify by delivering AcX selectively only into close proximity of the SNAP-tag coupled BG-TMR-MA. In this way, a large number of locally available monomers were provided for

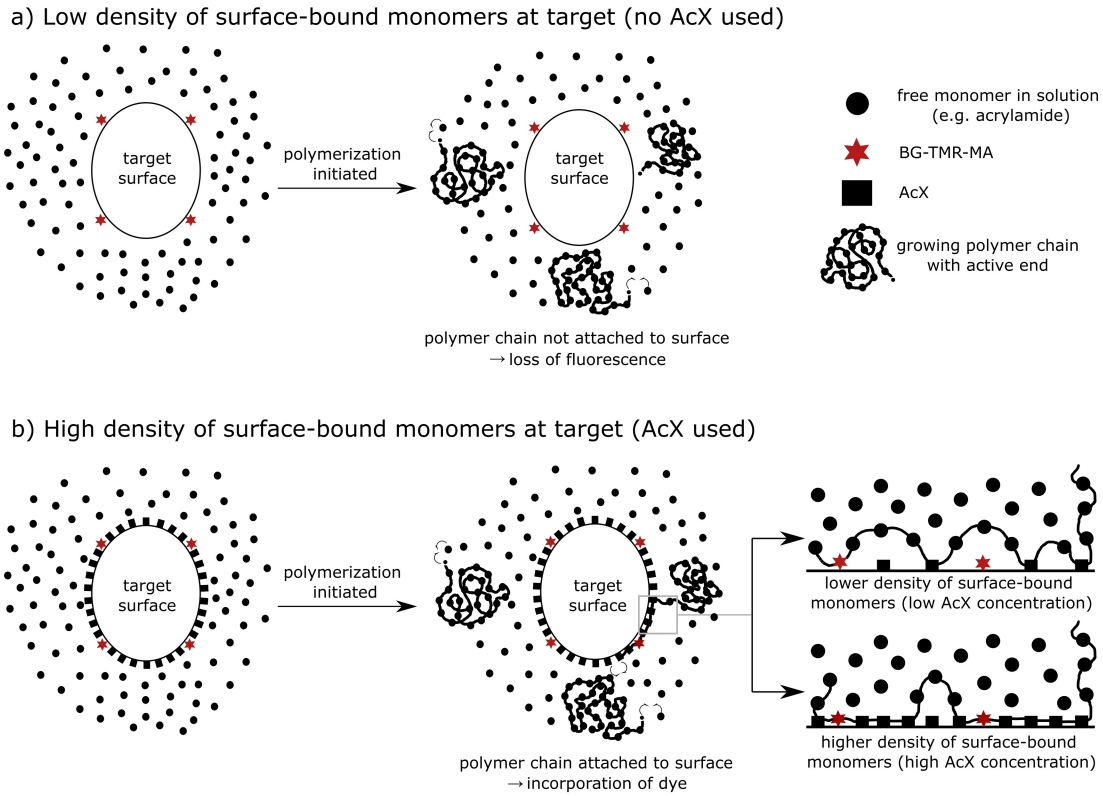

Figure 5. Model illustrating the role of surface grafting in dye retention. a) If no additional anchors like AcX are used, surface-bound monomers are only made up of BG-TMR-MA probes. The density of these monomers is too low for efficient embedding of the dye into the hydrogel. Once an active polymer chain end reaches the surface, it is unlikely that it encounters a surface-bound monomer. b) If the density of surface-bound monomers is significantly increased through the use of AcX, attachment of an active polymer chain end to the surface can take place. For increasing AcX concentrations, the probability of incorporating more surface-bound (and thus also more BG-TMR-MA) than free monomers increases.

efficient grafting of our dye into the gel, while alleviating the reduced expansion experienced in samples containing large amounts of AcX.

Our work thus demonstrates the relevance of monomer density, location and accessibility in the polymerization process in ExM. These considerations may help in future work when imaging large target structures with specific labeling approaches. Besides parameters affecting the target surface, further modifications on trifunctional probes may be carried out to optimize probe design and examine the influence of the monomer position at the label itself, e.g. by prolonging the linker between dye and monomer (at the cost of the labeling error), and the influence of the monomer density by introducing more monomers in the probe, as it has recently been shown by a different design approach for imaging RNA with ExM.[30] Our approach should be compatible with any fluorescent dye that withstands the polymerization and expansion procedure. The combination with the SNAP-tag offers significant advantages over immunofluorescence such as consistent kinetics of labeling for all targets it will be attached to and the possibility of using it for multicolor labeling of cells with other tags such as the HaLo-tag. On the other hand, it is incompatible with post-expansion staining, since the enzymatic activity is lost upon denaturing and thus may not allow for highest resolution staining due to labeling-error.

Conclusion

Our model, based on theory from polymer chemistry, provides new insights into ExM labeling strategy and should be beneficial for the design of ExM experiments in the future. Based on our model we propose to incorporate a strategy for "controlled grafting" into work with multifunctional dyes that bear polymerizable monomers. Additional reactive monomers should be made available close to the target in an additional step to ensure effective grafting of dyes into the gel. This may be possible by global addition of a crosslinker such as AcX or by directed delivery of AcX to the target structure as we demonstrate here.

We furthermore show that we can create exceptionally close covalent attachment to the target with a robust dye and incorporate it directly into the hydrogel in expansion microscopy in a single molecule smaller than 1 kDa. Our labeling was sufficient to allow for subdiffraction imaging of nuclear pores in a spinning disc confocal microscope at a level of maximally 32 dye molecules per nuclear pore. In providing stoichiometric labeling of single SNAP-tagged proteins with

single dyes and a strategy for their retention in the gel our work provides an essential step towards quantitative single molecule microscopy in combination with ExM.

Supporting Information

Respective characterization of compounds including spectral properties (Figure S1), comparison of Post-ExM images between SNAP-cell TMR-Star and BG-TMR-MA without addition of AcX (Figure S2), comparison of confocal images between BG-TMR-Boc and BG-TMR-MA (Figure S3), comparison between anchored and non-anchored fragments (Figure S4), diameter of nuclear pores in dependence of AcX concentration (S5). Materials and Methods. (PDF)

Acknowledgements

The authors thank Jonas Ries from EMBL for sharing NUP96-SNAP and Mike Heilemann from University Frankfurt for sharing NUP43-GFP stable cell lines. We would like to acknowledge the assistance of the Core Facility BioSupraMol supported by the DFG. RT and HE were supported by the Virocarb RTG 2327 of the Deutsche Forschungsgemeinschaft. IHB thanks the Studienstiftung des deutschen Volkes and the Dahlem Research School for PhD scholarships. The authors acknowledge support from Carlo Fasting. The authors thank all members of the Ewers and Haag laboratories for helpful discussions. The plasmid containing SNAP-CLC-YFP was a gift from Xiaowei Zhuang (Addgene plasmid # 38011). Open Access funding enabled and organized by Projekt DEAL.

Conflict of Interest

The authors declare no conflict of interest.

Data Availability Statement

The data that support the findings of this study are available from the corresponding author upon reasonable request.

Keywords: Expansion Microscopy · Grafting · SNAP-Tag · Super-Resolution Microscopy · Trifunctional Probe

[1] F. Chen, P. W. Tillberg, E. S. Boyden, *Science* **2015**, *347*, 543–548.
[2] S. Truckenbrodt, M. Maidorn, D. Crzan, H. Wildhagen, S. Kabatas, S. O. Rizzoli, *EMBO Rep.* **2018**, *19*, e45836.
[3] D. Unnersjö-Jess, L. Scott, H. Blom, H. Brismar, *Kidney Int.* **2016**, *89*, 243–247.
[4] M. Gao, R. Maraspini, O. Beutel, A. Zehtabian, B. Eickholt, A. Honigmann, H. Ewers, *ACS Nano* **2018**, *12*, 4178–4185.
[5] A. R. Halpern, G. C. M. Alas, T. J. Chozinski, A. R. Paredez, J. C. Vaughan, *ACS Nano* **2017**, *11*, 12677–12686.
[6] F. U. Zwettler, S. Reinhard, D. Gambarotto, T. D. M. Bell, V. Hamel, P. Guichard, M. Sauer, *Nat. Commun.* **2020**, *11*, 3388.
[7] P. W. Tillberg, F. Chen, K. D. Piatkevich, Y. Zhao, C.-C. Yu, B. P. English, L. Gao, A. Martorell, H.-J. Suk, F. Yoshida, E. M. DeGennaro, D. H. Roossien, G. Gong, U. Seneviratne, S. R. Tannenbaum, R. Desimone, D. Cai, E. S. Boyden, *Nat. Biotechnol.* **2016**, *34*, 987–992.
[8] A. T. Wassie, Y. Zhao, E. S. Boyden, *Nat. Methods* **2019**, *16*, 33–41.
[9] K. Min, I. Cho, M. Choi, J.-B. Chang, *Methods* **2020**, *174*, 3–10.
[10] T. Ku, J. Swaney, J.-Y. Park, A. Albanese, E. Murray, J. H. Cho, Y.-G. Park, V. Mangena, J. Chen, K. Chung, *Nat. Biotechnol.* **2016**, *34*, 973–981.
[11] D. Gambarotto, F. U. Zwettler, M. Le Guennec, M. Schmidt-Cernohorska, D. Fortun, S. Borgers, J. Heine, J.-G. Schloetel, M. Reuss, M. Unser, E. S. Boyden, M. Sauer, V. Hamel, P. Guichard, *Nat. Methods* **2019**, *16*, 71–74.
[12] G. Wen, M. Vanheusden, A. Acke, D. Valli, R. K. Neely, V. Leen, J. Hofkens, *ACS Nano* **2020**, *14*, 7860–7867.
[13] X. Shi, Q. Li, Z. Dai, A. A. Tran, S. Feng, A. D. Ramirez, Z. Lin, X. Wang, T. T. Chow, J. Chen, D. Kumar, A. R. McColloch, J. F. Reiter, E. J. Huang, I. B. Seiple, B. Huang, *J. Cell Biol.* **2021**, *220*, e202105067.
[14] M. Kang, J. Lee, S. Ko, S. Shim, *ChemBioChem* **2021**, *22*, 1396–1399.
[15] L. Yao, L. Zhang, Y. Fei, L. Chen, L. Mi, J. Ma, *Front. Chem.* **2021**, *9*, 303.
[16] D. Sun, X. Fan, Y. Shi, H. Zhang, Z. Huang, B. Cheng, Q. Tang, W. Li, Y. Zhu, J. Bai, W. Liu, Y. Li, X. Wang, X. Lei, X. Chen, *Nat. Methods* **2021**, *18*, 107–113.
[17] T. Schlichthaerle, M. T. Strauss, F. Schueder, A. Auer, B. Nijmeijer, M. Kueblbeck, V. Jimenez Sabinina, J. V. Thevathasan, J. Ries, J. Ellenberg, R. Jungmann, *Angew. Chem. Int. Ed.* **2019**, *58*, 13004–13008.
[18] J. Ries, C. Kaplan, E. Platonova, H. Eghlidi, H. Ewers, *Nat. Methods* **2012**, *9*, 582–584.
[19] T. J. Chozinski, A. R. Halpern, H. Okawa, H.-J. Kim, G. J. Tremel, R. O. L. Wong, J. C. Vaughan, *Nat. Methods* **2016**, *13*, 485–488.
[20] M. Beija, C. A. M. Afonso, J. M. G. Martinho, *Chem. Soc. Rev.* **2009**, *38*, 2410.
[21] J. V. Thevathasan, M. Kahnwald, K. Cieśliński, P. Hoess, S. K. Peneti, M. Reitberger, D. Heid, K. C. Kasuba, S. J. Hoerner, Y. Li, Y.-L. Wu, M. Mund, U. Matti, P. M. Pereira, R. Henriques, B. Nijmeijer, M. Kueblbeck, V. J. Sabinina, J. Ellenberg, J. Ries, *Nat. Methods* **2019**, *16*, 1045–1053.
[22] A. Szymborska, A. de Marco, N. Daigle, V. C. Cordes, J. A. G. Briggs, J. Ellenberg, *Science* **2013**, *341*, 655–658.
[23] C. M. Winterflood, H. Ewers, *ChemPhysChem* **2014**, *15*, 3447–3451.
[24] L. Pesce, M. Cozzolino, L. Lanzanò, A. Diaspro, P. Bianchini, *J. Biophotonics* **2019**, *12*, e201900018.
[25] P. Datta, J. Genzer, *J. Polym. Sci. Part A* **2016**, *54*, 263–274.
[26] D. Roy, M. Semsarilar, J. T. Guthrie, S. Perrier, *Chem. Soc. Rev.* **2009**, *38*, 2046.
[27] J. D. Wallat, K. A. Rose, J. K. Pokorski, *Polym. Chem.* **2014**, *5*, 1545–1558.
[28] S. A. Isarov, J. K. Pokorski, *ACS Macro Lett.* **2015**, *4*, 969–973.
[29] P. Datta, J. Genzer, *Macromolecules* **2013**, *46*, 2474–2484.
[30] G. Wen, M. Vanheusden, V. Leen, T. Rohand, K. Vandereyken, T. Voet, J. Hofkens, *J. Am. Chem. Soc.* **2021**, *143*, 13782–13789.

Manuscript received: February 15, 2023
Accepted manuscript online: May 9, 2023
Version of record online: May 26, 2023